Fluid Phase Equilibria xxx (2013) xxx–xxx

Contents lists available at ScienceDirect

Fluid Phase Equilibria

journal homepage: www.elsevier.com/locate/fluid

SAFT model for upstream asphaltene applications☆

Sai R. Panuganti[a], Mohammad Tavakkoli[a,b], Francisco M. Vargas[a,c], Doris L. Gonzalez[d], Walter G. Chapman[a,*]

[a] Department of Chemical and Biomolecular Engineering, Rice University, Houston, USA
[b] Department of Chemical and Petroleum Engineering, Sharif University of Technology, Tehran, Iran
[c] Department of Chemical Engineering, The Petroleum Institute, Abu Dhabi, UAE
[d] Fluid Specialist, BP, Houston, USA

ARTICLE INFO

Article history:
Received 22 March 2013
Received in revised form 14 May 2013
Accepted 16 May 2013
Available online xxx

Keywords:
Flow assurance
Asphaltene
PC-SAFT
Phase behavior

ABSTRACT

The increasing incidence of flow assurance problems caused by asphaltene deposition during oil production has motivated the development of numerous theoretical models and experimental methods to analyze this complex phenomenon. Even more challenging are the prediction of the occurrence and the magnitude of asphaltene deposition. It is well accepted that precipitation of asphaltene is a necessary condition for deposition. Hence, a significant amount of work has been devoted to the understanding of the conditions at which asphaltene precipitate from the crude oil. Although, several models seem to work well for correlating available data of onsets of asphaltene precipitation, they usually lack good prediction capabilities.

This article briefly reviews the properties of asphaltene and presents a thermodynamic model based on the Perturbed Chain version of the Statistical Associating Fluid Theory (PC-SAFT) equation of state, which is then proven to provide excellent prediction capabilities for the phase behavior of complex and polydisperse systems such as asphaltene, in a wide range of temperature, pressures and composition. Furthermore, several case studies are presented where the effect of gas injection, commingling of oils, and contamination with oil based mud, as well as the effect of asphaltene polydispersity are analyzed. Finally, the asphaltene compositional grading that can lead in some cases to the formation of tar-mat is studied using the same thermodynamic model. In all the cases, very good agreement with experimental data and field observations is obtained. From the results presented in this work, we are confident that the PC-SAFT equation of state is an excellent tool to understand the thermodynamic behavior of asphaltene in petroleum systems.

1. Introduction

Asphaltene are of particular interest to the petroleum industry because of their deposition tendencies in production equipment that cause considerable production costs. In addition, precipitated asphaltene impart high viscosity to crude oils, negatively impacting production. Unlike wax and gas hydrates, asphaltene pose a special challenge because asphaltene are not well characterized and can deposition even at high temperature. Aspects like light oils (very low in asphaltene content and easy to flow) reporting more asphaltene deposition problems than heavy oils (high in asphaltene content and difficult to flow), makes the problem even more interesting. Thus, the ability to predict thermodynamic and transport properties of crude oil systems containing asphaltene are important in planning for and possibly eliminating asphaltene related flow assurance problems.

In the second section of this paper, the properties of asphaltene fraction of a crude oil are reviewed. Based on this background and with the advances in asphaltene science, the solubility theory with liquid–liquid equilibrium using a SAFT based equation of state (EoS) is chosen as the most appropriate to model the thermodynamics of asphaltene. The third section of this paper explains SAFT and in particular the PC-SAFT equation of state with all the parameters required to predict the phase behavior of high molecular weight fluids such as asphaltene. The fourth section of this paper reviews

Abbreviations: SAFT, statistical associating fluid theory; PC-SAFT, perturbed chain form of the statistical associating fluid theory; EoS, equation of state; STO, stock tank oil; SARA, saturates, aromatics, resins and asphaltene; GOR, gas-to-oil ratio; AOP, asphaltene onset pressure; TLC-FID, thin layer chromatography with flame ionization detection; HPLC, high pressure liquid chromatography; OBM, oil based mud.

☆ This invited paper was presented in a special session at the AIChE 1st International Conference on Upstream Engineering and Flow Assurance (1st ICUEFA) held in Houston, Texas, USA, 1–5 April, 2012.

* Corresponding author. Tel.: +1 713 348 4900.
E-mail addresses: sai@rice.edu (S.R. Panuganti), mohammad.tavakkoli@rice.edu (M. Tavakkoli), fvargas@pi.ac.ae (F.M. Vargas), doris.gonzalez@bp.com (D.L. Gonzalez), wgchap@rice.edu (W.G. Chapman).

0378-3812/$ – see front matter © 2013 Elsevier B.V. All rights reserved.
http://dx.doi.org/10.1016/j.fluid.2013.05.010

Nomenclature

δ	solubility parameter
CED	cohesive energy density
U^{rsm}	residual internal energy
υ	pure liquid volume
RI	refractive index
n	concentration of asphaltene flocs
r	mean radius of aggregates
n_∞	final concentration of asphaltene flocs
R_∞	final mean radius of aggregates
t	time of aggregation
τ	characteristic time
A^{res}	residual Helmholtz free energy
$A^{segment}$	segment contribution to residual Helmholtz free energy
A^{chain}	chain contribution to residual Helmholtz free energy
A^{assoc}	association contribution to residual Helmholtz free energy
A_o^{hs}	hard-sphere contribution to residual Helmholtz free energy
A_o^{disp}	dispersion contribution to residual Helmholtz free energy
m	average segment number of the mixture
x_i	composition of species i
m_i	segment number of species i
R	universal gas constant
T	temperature
ρ	molecular number density
d_{ii}	temperature-dependent segment diameter of species i
σ_i	temperature-independent segment diameter of species i
I	system packing fraction function
η	package fraction
ε	segment–segment dispersion energy
k_{ij}	binary interaction parameter between species i and j
γ	aromaticity

the limitations of previous characterization procedures when applied for asphaltene, and hence the subsequent fifth section introduces a characterization methodology with asphaltene as one of the components in the crude oil. Results section include the successful PC-SAFT thermodynamic modeling and the understanding of asphaltene-crude oil system along with applications such as the analysis of a tar-mat which forms important organic barrier for an oil reservoir and must be modeled as accurately as possible in order to obtain correct estimate of producible reserves, effective placement of injection wells and ultimately, predictive production profiles.

2. Asphaltene background

Asphaltene are the polydisperse, heaviest and most polarizable fraction of crude oil. The term asphaltene was first introduced by Boussignault in 1837 to designate the material that precipitates out of petroleum upon addition of petroleum ether [1]. Today, it is operationally defined in terms of its solubility as the component of crude oil which is soluble in aromatic solvents, such as benzene, toluene or xylenes, but insoluble in light paraffinic solvents, such as n-pentane or n-heptane. The following aspects discuss the asphaltene properties.

2.1. Chemical composition

Asphaltene which are a solubility class of molecules found in crude oil; primarily consists of carbon, hydrogen, nitrogen, oxygen and sulfur, as well as trace amounts of iron, vanadium and nickel. An asphaltene molecule has a carbon number in the range of 40–80. The carbon to hydrogen ratio is approximately 1:1.2, depending on the asphaltene source [2].

2.2. Molecular structure

Asphaltene are polydisperse in nature, and hence do not have a specific chemical identity. In fairly early stages (1970s) of asphaltene research, Yen proposed a condensed aromatic cluster model that assumes extensive condensation of aromatic rings into large sheets with substitute side chains [3]. This type of structure was developed based on spectroscopic studies. Later on, a very different structural organization, the bride aromatic model is proposed by Murgich and Abaner based on structural mechanics [4]. A number of other investigators also attempted to postulate model structures for asphaltene including the recently proposed Modified Yen Model and a model presented by Vargas [5–7].

The first macrostructure of an asphaltene was proposed by Dickie and Yen in 1961 and is more popularly known as the Yen model [8]. Over the past decade, asphaltene science progressed dramatically and the Modified Yen Model proposed by Mullins in 2010 explained some more of the observed phenomena for asphaltene. According to the Modified Yen model, predominant part of an asphaltene structure consists of a single and moderately large polycyclic aromatic hydrocarbon, with peripheral alkanes. Asphaltene molecules form asphaltene nano-aggregates with aggregation numbers of ~6 and these aggregates can further cluster with aggregation numbers estimated to be ~8. More recently Vargas proposed an asphaltene structural model also incorporating the aging effects, and thereby designed a new type of asphaltene deposition inhibitor with preliminary success.

2.3. Molecular weight

Depending on the solvent, concentration and the measurement technique employed, several molecular weight ranges are reported for asphaltene. Different techniques used to estimate the molecular weight of asphaltene include vapor-pressure osmometry, viscometry, boiling point elevation, freezing point depression, light scattering, gel permeation chromatography, florescence depolarization, ultracentrifuge, electron microscope studies. The vapor-pressure osmometry technique results in an asphaltene molecular weight in the range of 800–3000 g/mol in good solvents [9]. Alboudwarej et al. estimated an average molecular weight of asphaltene as 1800 g/mol for heavy oil and bitumen [10]. Adopting the Modified Yen Model, Zuo et al. concluded the molecular weight of asphaltene nanoaggregate as ~1600 g/mol [11]. Long before the Modified Yen Model, in 1984 Hirschberg and Hermans estimated the average asphaltene molecular weight to be between 1300 and 1800 g/mol based on phase behavior studies [12].

2.4. Density

The density of petroleum derived asphaltene at ambient conditions varies between 1.1 and 1.2 g/cm^3 based on the origin and methodology [13–15]. Diallo et al. estimated an average asphaltene density as 1.12 g/cm^3 based on (NPT) isothermal isobaric ensemble dynamic molecular simulations followed by energy minimization

Please cite this article in press as: S.R. Panuganti, et al., SAFT model for upstream asphaltene applications, Fluid Phase Equilib. (2013), http://dx.doi.org/10.1016/j.fluid.2013.05.010

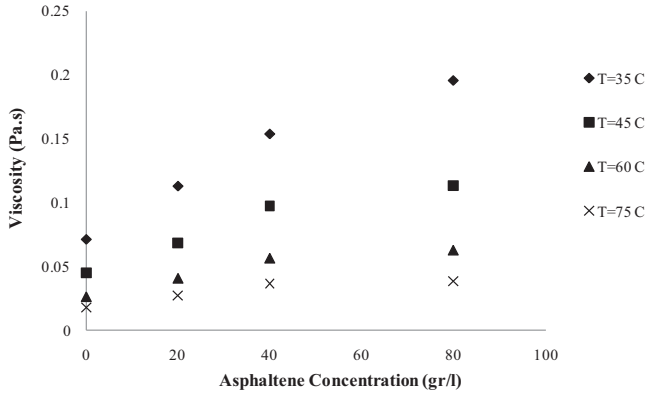

Fig. 1. Effect of asphaltene concentration on slurry sample viscosity at different temperature.

[16]. This estimated density compares favorably with the measured density, 1.16 g/cm^3 of petroleum asphaltene reported by Yen et al. using helium displacement [17].

2.5. Diffusion

Asphaltene diffusion coefficient is a function of concentration dependent size of the asphaltene aggregates. At low concentration, the degree of association of asphaltene is small, but increases with increase in concentration until a critical size is reached. The higher the state of association, the larger the entity size and lower the diffusion coefficient. The diffusion coefficient of asphaltene in toluene estimated by low field nuclear magnetic resonance and florescence spectroscopy measurements is in the order of 10^{-10} m^2/s for a particle size of 1–2 nm [18]. The diffusion coefficient in toluene at infinite asphaltene dilution is 2.2×10^{-10} m^2/s [19].

2.6. Interfacial characteristics

The oil–water interfacial properties in the presence of asphaltene are peculiar. The initial rapid diffusion of asphaltene towards the interface is followed by a long reorganization and progressive building of layers. The overall adsorption process is slow, but for different oils, has similar time scales [20]. When asphaltene concentration is varied, interfacial equilibrium is reached faster at higher asphaltene concentration for good solvents and slower in the presence of poor solvents. Asphaltene molecules also adsorb at oil–air interface, forming skins which impart stability to foamy oils in which bubbles persist for long duration of time [21,22].

In the presence of surfactant there is a co-adsorption of both surfactant and asphaltene at the oil–water interface. Surfactants being smaller molecules than asphaltene arrive at the interface before the arrival of asphaltene. At intermediate times, surface population is over compressed by surfactants adsorbed at the interface and incoming asphaltene. This over-population of the surface gives rise to a minimum in the dynamic surface tension [20]. At long enough times, the interfacial tension increases with time, a phenomenon not seen with asphaltene or surfactant alone. Such a phenomenon indicates a transfer of species across the interface, at which location other species settle [23].

2.7. Viscosity

The presence of asphaltene means additional difficulties related to transport and processing due to an increased crude oil viscosity caused by the asphaltene. Our experimental results on asphaltene content and temperature affecting the crude oil viscosity are plotted in Fig. 1, where the slurry represents an Iranian crude oil containing asphaltene. The evidence of increased asphaltene content and low temperature significantly increasing the oil viscosity is already reported by Sirota et al. [24].

Presence of precipitated asphaltene particles results in an increase in the viscosity of the oil. This increase becomes remarkable at and after the onset of flocculation, and hence can be used to detect the asphaltene precipitation onset conditions [25]. Compositional grading is a well-known phenomenon and with asphaltene compositional variation, the crude oil viscosity changes significantly with depth. Modeling the crude oil viscosity variation with depth due to asphaltene compositional grading, can help in predicting the occurrence of a tar-mat, characterized as the highly viscous oil zone enriched in asphaltene [26].

2.8. Solubility parameter

Considering asphaltene as a soluble species, solubility parameter (δ) can be an important tool based on which asphaltene phase behavior can be explained. The solubility parameter for a non-polar fluid is given by Hildebrand as,

$$\delta = \sqrt{CED} = \sqrt{-\frac{U^{rsm}}{\upsilon}} \quad (1)$$

where, CED is the cohesive energy density, U^{rsm} is the residual internal energy obtained by subtracting the ideal gas contribution from that of the real fluid and υ is the pure liquid volume. Asphaltene has the highest solubility parameter among the crude oil components and is between 19 and 24 MPa$^{0.5}$ [27]. If asphaltene is assumed to be dissolved in crude oil, the equilibrium can be altered by a change in temperature, pressure or composition of the oil. For example, if significant amounts of low molecular weight hydrocarbons are dissolved into the liquid phase, the solubility parameter of oil is reduced and the asphaltene precipitate may form. Changes in temperature and pressure will likewise alter the solubility parameter, thus causing conditions that induce precipitation.

2.9. Refractive index

The refractive index (RI) of an asphaltene solution can be measured in place of the solubility parameter based on the observation that London dispersion interactions dominate the asphaltene phase behavior [28]. The London dispersion properties of a material can be characterized by the wavelength dependence of the refractive index or the "dispersion" of visible light. Refractive index and solubility parameter can be inter-converted, and at 20 °C the linear correlation 2 holds good. Using this equation, the refractive index of pure asphaltene is observed to range from 1.54 to 1.74.

$$\delta = 52.042\left(\frac{RI^2 - 1}{RI^2 + 2}\right) + 2.904 \quad (2)$$

2.10. Precipitation

Asphaltene precipitation is treated as the growth of primary particles from a solution due to super-saturation. Thus, asphaltene precipitation consumes super-saturation until the system reaches an equilibrium asphaltene concentration. Very limited data is available in the literature about the rate of asphaltene precipitation and the reported spectrophotometry data on 0.1 g of asphaltene/L of toluene and mixed with a 50 volume % n-heptane solution, can be approximately modeled using a first order precipitation rate constant of 0.01 min^{-1} [29].

2.11. Aggregation

Aggregation does not consume super-saturation and is considered as the agglomeration of primary particles forming larger,

Please cite this article in press as: S.R. Panuganti, et al., SAFT model for upstream asphaltene applications, Fluid Phase Equilib. (2013), http://dx.doi.org/10.1016/j.fluid.2013.05.010

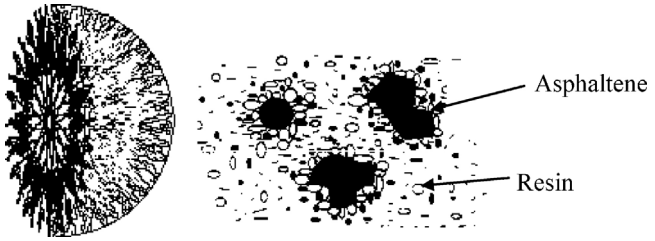

Fig. 2. Asphaltene colloidal model [39].

secondary particles (asphaltene aggregate). Concentration of asphaltene aggregates less than the critical micelle concentration of 3–4 g of asphaltene/L toluene is controlled by diffusion, while at higher asphaltene concentration the aggregation is controlled by impact [30]. Most of the available literature does not consider precipitation and aggregation separately. Researchers using microscopy define the onset of asphaltene precipitation based on the resolution limit of microscopes. The redissolution kinetics of precipitated asphaltene can be considerable in the time scale of well-bore travel, while that of aggregated asphaltene is slow and hence negligible [31]. It is experimentally observed that asphaltene aggregate particle size gets saturated with time and assuming exponential approach to equilibrium, Anisimov et al. obtained [31]:

$$nr^3 = n_\infty R_\infty^3 (1 - e^{-t/\tau}). \quad (3)$$

2.12. Deposition/adsorption

Photothermal surface deformation studies of asphaltene adsorption onto surfaces revealed that the adsorption resulted in multilayer formation [32]. Recent studies performed using quartz crystal microbalance showed saturation adsorption isotherms with rapid initial response followed by slow approach to equilibrium [33]. The initial response is indicative of a diffusion controlled process. At longer timescales, the data is found to follow first-order kinetics. The overall first order rate constant is estimated as $\sim 2 \times 10^{-3}$ min^{-1} [34]. But, all the above observations are reported for asphaltene solubilized in toluene and the adsorption kinetics of precipitated asphaltene can be to be different.

2.13. Asphaltene–crude oil system

Understanding of the asphaltene stability in crude oil is based mainly on two different thermodynamic models: colloidal and solubility models. The colloidal approach describes asphaltene phase behavior assuming that the crude oil can be divided into polar and non-polar subfractions or solvent in which resins stabilize asphaltene as in micelle formation [35]. The solubility model uses the molecular solubility approach to describe an asphaltene containing fluid as a mixture of solute (asphaltene) and solvent (bulk oil) in a homogeneous liquid state [36]. The asphaltene precipitation can be treated as solid–liquid or liquid–liquid equilibrium, and is reversible. But, as discussed in the *Aggregation* section, the kinetics of re-dissolution varies significantly depending on the physical state of the system.

The colloidal model assumes that asphaltene exist in the oil as solid particles; and, describes the stability of asphaltene in terms of micelle formation where asphaltene self-associate into an aggregate to form the core and resins adsorb onto the core (based on polar–polar interactions) to form a steric shell shown in Fig. 2. These points of view are based on the observation that an increase in resins content improves the stability of asphaltene. According to these models, asphaltene precipitates when a sufficient amount of diluent is added to the system because the concentration of resins is diluted, with resins becoming increasingly soluble in the liquid phase that separate them from the asphaltene micelles. However, the addition of solvents like toluene actually takes asphaltene back into solution. Using impedance analysis, Goual demonstrated that the diffusion coefficient of asphaltene is same in the presence and absence of resin [37]. Thus, resins are unlikely to coat asphaltene nanoaggregates and do not provide the steric stabilizing layer that the colloidal model proposes. Also, the polar nature of asphaltene is never confirmed in terms of charge carried by the asphaltene particles through hydrophilic–lipophilic balance [38]. While colloidal models of asphaltene were beneficial in the early stages of understanding asphaltene behavior, these analogies are not justified.

Solubility models assume that asphaltene is dissolved in the crude oil. This equilibrium can be solid–liquid or liquid–liquid type. In the solid–liquid type by Nghiem and Coombe [40], precipitated asphaltene is treated as a single component residing in the solid phase, while oil and gas phases are modeled with a cubic equation of state. However, pure asphaltene is never precipitated [41]. Also asphaltene is a substance with no defined melting point, high solubility parameter and moderately high molecular weight. Having a high aromatic content, it forms true solution in aromatic solvents. However, its molecular weight being moderately high, the entropy of mixing is not sufficient to keep it in solution if the interaction with remainder of the solution becomes unfavorable, such as upon the addition of an aliphatic fluid. The phase separation which results is thus thermodynamically driven liquid–liquid equilibrium.

The liquid–liquid treatment was initially proposed by Hirschberg, et al. [42] starting with a detailed compositional model based on the Soave equation of state to calculate liquid phase compositions and molar volumes before asphaltene precipitation. Then, using a Flory–Huggins-regular solution theory, the amount of precipitated asphaltene is estimated by calculating the solubility parameter from Hildebrand's definition. This initial approach is difficult to extend to model the asphaltene solubility under reservoir conditions, because the solubility parameters must be corrected with correlations or an equation of state for high pressure and temperature. Also cubic equation of state models cannot describe the phase behavior of systems with large size disparities and they cannot accurately describe their fluid densities.

A more modern equation of state is the Statistical Associating Fluid Theory family. This equation of state based on statistical mechanics can accurately model mixtures of different molecular sizes. Thus, solubility model with liquid–liquid equilibrium using a SAFT based equation of state is the most appropriate theory for modeling asphaltene phase behavior. SAFT based equations of state have demonstrated excellent performance and predictive capabilities applied to a wide range of mixtures, including petroleum systems [43].

3. SAFT theory

The statistical association fluid theory is a molecular-based equation of state derived by Chapman et al. by applying and extending Wertheim's first-order perturbation theory to chain molecules [44–46]. In this theory, molecules are modeled as chains of bonded spherical segments and the properties of a fluid are obtained by expanding about the same properties of a reference fluid. SAFT has a similar form to group contribution theories in that the fluid of interest is initially considered to be a mixture of unconnected groups or segments. As shown in Fig. 3, SAFT includes a chain connectivity term to account for the bonding of various groups to form polymers and an explicit association term to account for intermolecular attractions like hydrogen bonding.

Please cite this article in press as: S.R. Panuganti, et al., SAFT model for upstream asphaltene applications, Fluid Phase Equilib. (2013), http://dx.doi.org/10.1016/j.fluid.2013.05.010

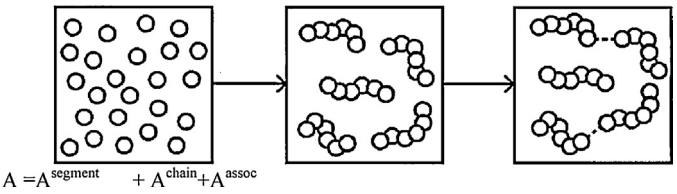

Fig. 3. SAFT treats molecules as chains of spherical segments. The fluid's free energy is then the sum of the independent segment free energy and the change in free energy due to chain formation and association.

SAFT describes the residual Helmholtz free energy (A^{res}) of a fluid as

$$A^{res} = A - A_{ideal} = A^{segment} + A^{chain} + A^{assoc} = m(A_o^{hs} + A_o^{disp}) + A^{chain} + A^{assoc} \quad (4)$$

where $A^{segment}$, A^{chain}, A^{assoc}, A_o^{hs} and A_o^{disp} are the segment, chain, association, hard-sphere, and dispersion contributions, respectively, to the mixture's residual Helmholtz free energy. The average segment number of the mixture, m, is an average of the pure species' segment number, m_i, weighted by the species' compositions, x_i.

$$m = \sum_i x_i m_i \quad (5)$$

The statistical association fluid theory and its various modifications and extensions have demonstrated the ability to accurately predict phase behavior of simple, hydrogen bonding, polar, and polymeric mixtures [47]. It is particularly useful for modeling systems with significant chain contribution effects (as in polymer mixtures). When considering asphaltene phase behavior dominated by nonpolar interactions, PC-SAFT is chosen among different forms of SAFT [48]. Gross and Sadowski proposed the perturbed chain modification (PC-SAFT) to account for the effects of chain length on the segment dispersion energy, by applying the Barker-Henderson perturbation theory truncated at the second-order term to a hard chain reference fluid [49]. PC-SAFT employs a hard sphere reference fluid described by the Mansoori-Carnahan-Starling-Leland equation of state. This version of SAFT properly predicts the phase behavior of mixtures containing high molecular weight components similar to the large asphaltene molecules.

The free energy contribution of the hard-sphere mixtures given by Mansoori-Carnahan-Starling-Leland equation of state is [50]

$$\frac{A_o^{hs}}{RT} = \frac{6}{\pi\rho}\left[\frac{\zeta_2^2 + 3\zeta_1\zeta_2\zeta_3 - 3\zeta_1\zeta_2\zeta_3^2}{\zeta_3(1-\zeta_3)^2} - \zeta_0\left(1 - \frac{\zeta_2^3}{\zeta_3^2}\right)\ln(1-\zeta_3)\right] \quad (6)$$

where

$$\zeta_k = \frac{\pi\rho}{6}\sum_i x_i m_i d_{ii}^k \quad (7)$$

and

$$d_{ii}^k = \sigma_i\left[1 - 0.12\exp\left(\frac{-3u_i}{kT}\right)\right] \quad (8)$$

Here, ρ is the number density (molecules/A^3), d_{ii} the temperature-dependent segment diameter of species i in units of Angstroms and σ_i is the adjustable PC-SAFT temperature independent segment diameter (A). A temperature dependent hard sphere diameter accounts for the soft repulsion between molecules. Calculated for Barker-Henderson theory, the temperature dependence is fit by Chen and Kerglewski [51].

The contribution to free energy due to chain formation from Wertheim theory is given by [46]

$$\frac{A^{chain}}{RT} = \sum_i x_i(1-m_i)\ln g_{ii}^{hs}(d_{ii}) \quad (9)$$

where

$$g_{ii}^{hs}(d_{ii}) = \left[\frac{1}{1-\zeta_3} + \frac{3d_{ii}\zeta_2}{2(1-\zeta_3)^2} + \frac{d_{ii}^2\zeta_2^2}{2(1-\zeta_3)^3}\right] \quad (10)$$

Perturbed chain version of SAFT was initially developed for alkanes by incorporating the effects of chain length on the segment dispersion energy. With PC-SAFT, the dispersion contribution becomes [49]

$$\frac{A_o^{disp}}{RT} = \frac{A_1}{RT} + \frac{A_2}{RT} \quad (11)$$

$$\frac{A_1}{RT} = -2\pi\rho I_1(\eta, m)\sum_i\sum_j \frac{x_i x_j m_i m_j \sigma_{ij}^3 \varepsilon_{ij}}{kT} \quad (12)$$

$$\frac{A_2}{RT} = -2\pi m I_2(\eta, m) W^{-1}\sum_i\sum_j \frac{x_i x_j m_i m_j \sigma_{ij}^3 \varepsilon_{ij}^2}{(kT)^2} \quad (13)$$

$$W = 1 + m\frac{8\eta - 2\eta^2}{(1-\eta)^4} + (1-m)\frac{20\eta - 27\eta^2 + 12\eta^3 - 2\eta^4}{(1-\eta)^2(2-\eta)^2} \quad (14)$$

$$\varepsilon_{ij} = (1-k_{ij})\sqrt{\varepsilon_{ii}\varepsilon_{jj}} \quad (15)$$

$$\sigma_{ij} = \frac{\sigma_i + \sigma_j}{2} \quad (16)$$

where η is the package fraction, I_1 and I_2 are functions of the system packing fraction, ε is the segment–segment dispersion energy and k_{ij} is the binary interaction parameter between species i and j. Eq. (11) is derived from Barker–Henderson perturbation theory, and A_1 and A_2 correspond to the first and second order contributions, respectively [52]. Reexamining the equations from 6 to 16, it is observable that in PC-SAFT for pure components only three parameters are required to be estimated, which are the number of segments per molecule (m), the temperature-independent diameter of each molecular segment (σ) and the segment–segment dispersion energy (ε). Although PC-SAFT requires only three parameters, the equation of state produces accurate vapor pressures and liquid densities. Cubic equations of state with volume translation typically require four or more pure component parameters to fit the same data.

The main presumption in the PC-SAFT approach for the thermodynamic modeling of asphaltene is that asphaltene associate to form preaggregates and further association is not considered during precipitation. Therefore, asphaltene phase behavior can be qualitatively explained in terms of London dispersion interactions, and the polar interactions are assumed to have an insignificant contribution. Aromatic ring compounds making the core of asphaltene are highly polarizable; therefore, polarizability determines the ability of hydrocarbons to serve as a precipitant or as a solvent for asphaltene. The evidence obtained through the works of Buckley and Hirasaki validates the presumption that polarity does not play a significant role in asphaltene phase behavior [28,53]. Thus the association term in SAFT can be safely neglected for asphaltene thermodynamic modeling.

4. Characterization of reservoir fluid

Crude oil has numerous components and characterizing the oil as a mixture of well-defined fractions that represent blends of similar components instead of handling the components individually, will aid in reducing the computational cost significantly. The earliest study on crude oil characterization dates back to 1978 by Katz and Firoozabadi [54] where the boiling point temperature of n-paraffins are used for separating the carbon number fraction. The resulting densities are for paraffinic oils and therefore very low [55].

Please cite this article in press as: S.R. Panuganti, et al., SAFT model for upstream asphaltene applications, Fluid Phase Equilib. (2013), http://dx.doi.org/10.1016/j.fluid.2013.05.010

Table 1
Compositional analysis of crude oil A.

Component	MW (g/mol)	Density (g/cm^3)	Flashed gas		STO		Reservoir fluid (GOR-787 scf/stb)	
			wt%	mol%	wt%	mol%	wt%	mol %
N_2	28.04	0.809	0.270	0.280	0	0	0.047	0.163
CO_2	44.01	0.817	5.058	3.340	0	0	0.874	1.944
H_2S	34.08	0.786	0	0	0	0	0	0
C_1	16.04	0.300	31.858	57.716	0	0	5.503	33.600
C_2	30.07	0.356	13.431	12.981	0.044	0.279	2.356	7.557
C_3	44.10	0.508	17.571	11.581	0.296	1.294	3.280	6.742
iC_4	58.12	0.567	5.280	2.640	0.251	0.835	1.120	1.884
nC_4	58.12	0.586	11.74	5.871	0.923	3.066	2.792	4.695
iC_5	72.15	0.625	4.593	1.850	0.999	2.673	1.620	2.195
nC_5	72.15	0.631	5.139	2.070	1.589	4.250	2.202	2.984
C_6	84.00	0.690	3.497	1.210	3.593	8.254	3.576	4.162
Mcyclo-C_5	84.16	0.749	0	0	0.447	1.024	0.369	0.429
Benzene	78.11	0.876	0	0	0.143	0.354	0.119	0.148
Cyclo-C_6	84.16	0.779	0	0	0.322	0.739	0.267	0.310
C_7	96.00	0.727	1.222	0.370	3.604	7.245	3.193	3.251
Mcyclo-C_6	98.19	0.770	0	0	0.619	1.217	0.512	0.510
Toluene	92.14	0.867	0	0	0.702	1.471	0.581	0.616
C_8	107.00	0.749	0.258	0.070	3.805	6.862	3.192	2.916
C_2-Benzene	106.17	0.866	0	0	0.224	0.407	0.185	0.171
m&p Xylene	106.17	0.860	0	0	0.644	1.171	0.533	0.491
o Xylene	106.17	0.860	0	0	0.038	0.069	0.032	0.029
C_9	121	0.768	0.083	0.020	3.936	6.277	3.270	2.642
C_{10}	134	0.782	0	0	4.605	6.632	3.809	2.779
C_{11}	147	0.793	0	0	3.787	4.971	3.132	2.083
C_{12}	161	0.804	0	0	3.241	3.885	2.682	1.628
C_{13}	175	0.815	0	0	3.096	3.414	2.561	1.431
C_{14}	190	0.826	0	0	2.929	2.975	2.423	1.247
C_{15}	206	0.836	0	0	2.83	2.651	2.341	1.111
C_{16}	222	0.843	0	0	2.437	2.150	2.046	0.901
C_{17}	237	0.851	0	0	2.356	1.918	1.949	0.804
C_{18}	251	0.856	0	0	2.128	1.636	1.761	0.686
C_{19}	263	0.861	0	0	2.231	1.637	1.845	0.686
C_{20}	275	0.866	0	0	2.193	1.539	1.814	0.645
C_{21}	291	0.871	0	0	1.900	1.260	1.572	0.528
C_{22}	300	0.876	0	0	1.805	1.161	1.493	0.486
C_{23}	312	0.881	0	0	1.628	1.007	1.346	0.422
C_{24}	324	0.885	0	0	1.512	0.900	1.250	0.377
C_{25}	337	0.888	0	0	1.417	0.811	1.172	0.340
C_{26}	349	0.892	0	0	1.377	0.761	1.139	0.319
C_{27}	360	0.896	0	0	1.269	0.680	1.050	0.285
C_{28}	372	0.899	0	0	1.280	0.664	1.059	0.278
C_{29}	382	0.902	0	0	1.079	0.545	0.893	0.228
C_{30}	394	0.903	0	0	1.031	0.505	0.853	0.212
C_{31}	404	0.907	0	0	0.937	0.448	0.775	0.188
C_{32}	415	0.910	0	0	0.883	0.411	0.731	0.172
C_{33}	426	0.913	0	0	0.803	0.364	0.664	0.152
C_{34}	437	0.916	0	0	0.694	0.307	0.574	0.129
C_{35}	445	0.919	0	0	0.666	0.289	0.551	0.121
C_{36}+	594	0.941	0	0	27.673	8.991	22.893	3.767

A later method proposed by Whitson, as a correction of Katz and Firoozabadi, is widely applied in the industry to characterize the stock tank oil (STO) [56]. Whitson's method is based on the average boiling point of each single carbon number cut and correlations from Riazi and Daubert [57]. Whitson's method presents a set of physical properties for the petroleum fractions C_6 through C_{45}. The calculated properties include average boiling point, specific gravity, and molecular weight based on an analysis of the physical properties of liquid hydrocarbons and condensates. However, this characterization method leads to significant errors when applied to heavier components [58].

Whitson's method is followed by the paraffins-naphthenes-aromatics method to characterize crude oil liquid phase. A new set of correlations reported by Riazi on the properties of single carbon number from C_6 to C_{50} is used to estimate the paraffins-naphthenes-aromatics composition [59]. Leelavanichkul et al. used the paraffins-naphthenes-aromatics technique to characterize different hydrocarbon fluids in a solid–liquid model to determine the asphaltene precipitation onsets [60]. However, the solubility parameter for C_{50} fraction is low to represent the heaviest fractions in a crude oil. Also, the maximum refractive index does not reach the expected 1.7 value that has been estimated for asphaltene [53].

Even with the availability of the SAFT models in commercial simulators such as PVT Sim, Multiflash and VLXE, the lack of a standard characterization procedure incorporating the heavy components such as asphaltene, hinders the industrial use of SAFT based models for asphaltene applications [61].

5. Characterization methodology

The characterization procedure described below is based on saturates-aromatics-resins and-asphaltene (SARA) analysis of stock tank oil. A reservoir fluid which is usually monophasic, when flashed from reservoir to ambient conditions yields residual liquid/stock tank oil and an evolved gas phase/flashed gas. Such a flash of reservoir fluid is carried out under controlled environment in a PVT cell, and the liberated gas and residual liquid are analyzed for composition using gas chromatography. Table 1 reports the

Please cite this article in press as: S.R. Panuganti, et al., SAFT model for upstream asphaltene applications, Fluid Phase Equilib. (2013), http://dx.doi.org/10.1016/j.fluid.2013.05.010

Table 2
Properties of crude oil A.

GOR (scf/stb)	787
MW of reservoir fluid (g/mol)	97.750
MW of flashed gas (g/mol)	29.06
MW of STO (g/mol)	192.99
STO Density (g/cm^3)	0.82
Saturates (wt%)	66.26
Aromatics (wt%)	25.59
Resins (wt%)	5.35
Asphaltene (wt%)	2.80

Table 3
PC-SAFT parameter correlations for saturates as a function of molecular weight.

Parameter	Function
m	$(0.0257 \times MW) + 0.8444$
$\sigma(A)$	$4.047 - \frac{4.8013 \times \ln(MW)}{MW}$
$\varepsilon(K)$	$\exp\left(5.5769 - \frac{9.523}{MW}\right)$

Table 4
Characterized gas phase for crude oil A.

Component	MW (g/mol)	mole (%)	PC-SAFT parameters		
			m	σ (A)	ε (K)
N_2	28.01	0.28	1.21	3.31	90.96
CO_2	44.01	3.34	2.07	2.78	169.21
C_1	16.04	57.72	1.00	3.70	150.03
C_2	30.07	12.98	1.61	3.52	191.42
C_3	44.10	11.58	2.00	3.62	208.11
Heavy gas	65.49	14.10	2.53	3.74	228.51

compositional analysis of crude oil A and Table 2 shows the properties of crude oil A which is used for describing the characterization.

It is well known that the light components in oil affect both bubble pressure and asphaltene onset pressure (AOP) significantly. Hence, considering the lightest fractions of oil individually will result in better prediction of asphaltene onset pressures. Thus gas phase is characterized to consist of seven components: N_2, CO_2, methane, ethane, propane and heavy gas pseudo-component that represents a mixture of hydrocarbons heavier than propane. The PC-SAFT equation of state parameters for the pure components, N_2, CO_2 and C_1–C_3, are available in literature [49]. The average molecular weight of the heavy gas pseudo-component (mostly consisting of saturates) is used to estimate the corresponding PC-SAFT parameters through correlations shown in Table 3 [62]. Table 4 represents the characterized gas phase of crude oil A. If H_2S is also present in the flashed gas, the number of components in the characterized gas phase will become eight with H_2S being considered individually.

The liquid fraction characterization into saturates, aromatics plus resins and asphaltene is based on stock tank oil composition and SARA analysis. Because of their similar thermodynamic effect on the asphaltene phase behavior, the aromatics and resin fractions are combined into a single lumped pseudo component defined in terms of the degree of aromaticity (γ). Table 5 shows the PC-SAFT parameters for the aromatics + resins pseudo fraction [62]. The aromaticity parameter determines the aromatics plus resins tendency

Table 5
PC-SAFT parameter correlations for aromatics + resins pseudo component as a function of molecular weight. The equations are of the form, Parameter = $(1-\gamma)$(Benzene derivatives correlation) + γ(Poly-nuclear-aromatic correlation).

Parameter	Function
m	$(1-\gamma)(0.0223 \times MW + 0.751) + \gamma(0.0101 \times MW + 1.7296)$
$\sigma(A)$	$(1-\gamma)\left(4.1377 - \frac{38.1483}{MW}\right) + \gamma\left(4.6169 - \frac{93.98}{MW}\right)$
$\varepsilon(K)$	$(1-\gamma)(0.00436 \times MW + 283.93) + \gamma\left(508 - \frac{234100}{(MW)^{1.5}}\right)$

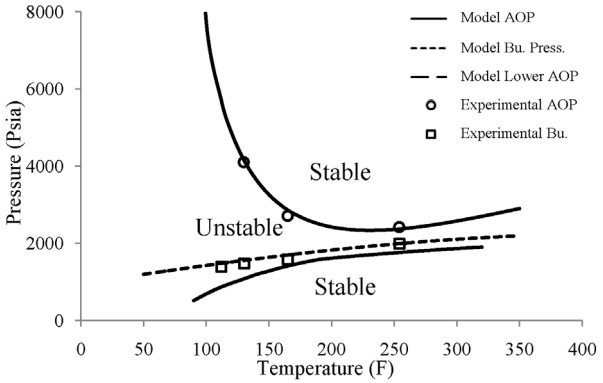

Fig. 4. Asphaltene phase envelope for crude oil A generated by PC-SAFT.

to behave as poly-nuclear-aromatic ($\gamma = 1$) or benzene derivative ($\gamma = 0$), and is tuned to meet the values of density and bubble point simultaneously for the entire oil.

Asphaltene exist as pre-aggregated molecules even in good solvents such as toluene, and the average molecular weight for such a pre-aggregated asphaltene is considered as 1700 g/mol [11,48,63]. The asphaltene PC-SAFT parameters in the recombined oil are tuned to meet the onset of asphaltene precipitation. Table 6 shows the characterized stock tank oil before recombining. The gas phase and stock tank oil are then recombined as per the gas-to-oil ratio (GOR) at reservoir conditions or the monophasic fluid molecular weight, and Table 7 represents the characterized live oil after tuning the parameters. The constant set of temperature independent PC-SAFT binary interaction parameters are well established through one of our recent works, by fitting to binary vapor–liquid equilibrium data for a combination of pure components [64]. Further tuning of the binary interaction parameters may be necessary based on the individual case. With all the pseudo components and parameters set, PC-SAFT can be used like any other equation of state and Fig. 4 plots the resultant asphaltene phase behavior of crude oil A. For all the oils discussed in this article, the characterized fluids along with PC-SAFT parameters are reported in the supplementary material.

An asphaltene onset condition is the cloud point at a fixed temperature for which the crude oil will split up into two liquid phases of asphaltene rich and lean phases. Such measurements can involve depressurization of live oil or titration with a precipitant. The lower asphaltene onset represents the pressure below which asphaltene and oil coexist in a single phase.

Recently Punnapala and Vargas showed that the number of adjusted parameters of asphaltene can be reduced to two from three by estimating molecular weight and aromaticity of the asphaltene instead of the three PC-SAFT parameters [65]. For this work aromaticity is redefined as 0 for saturates and 1 for polynuclear aromatics. For asphaltene, aromaticity and molecular weight are fitted to match the asphaltene onset data reported by either NIR depressurization experiments or n-alkane titrations at ambient conditions.

In either of the methods, one of the important inputs on which a crude oil is characterized is the SARA. Unfortunately, a disadvantage of SARA analysis is that fraction measurements by different techniques can show large differences [66,67]. Table 8 shows the SARA reported by thin layer chromatography with flame ionization detection (TLC-FID) and high pressure liquid chromatography (HPLC) for the same light crude oil B. In the process of quantifying SARA, TLC-FID lost significant amount of light ends, and hence reported a higher amount of aromatics and asphaltene than actually present. When the SARA measured by the same lab for another light crude oil C from a different field in the same region is made available through TLC-FID, the corrected weight fractions are obtained

Please cite this article in press as: S.R. Panuganti, et al., SAFT model for upstream asphaltene applications, Fluid Phase Equilib. (2013), http://dx.doi.org/10.1016/j.fluid.2013.05.010

Table 6
Characterized stock tank oil for crude oil A.

Component	MW (g/mol)	mole%	PC-SAFT parameters		
			m	σ (A)	ε (K)
Saturates	167.68	75.97	5.15	3.90	249.69
Aromatics + Resins (γ = to be tuned)	253.79	23.71	6.41	3.99	285.00
Asphaltene	1700	00.32	To be tuned	To be tuned	To be tuned

Table 7
Characterized crude oil A.

Component	MW (g/mol)	Contribution from gas	Contribution from STO (moles)	Moles in live oil	PC-SAFT parameters		
		Moles		Basis 100	m	σ (A)	ε (K)
N_2	28.04	0.163	0	0.163	1.21	3.31	90.96
CO_2	44.01	1.944	0	1.944	2.07	2.78	169.21
C_1	16.04	33.600	0	33.600	1.00	3.70	150.03
C_2	30.07	7.557	0	7.557	1.61	3.52	191.42
C_3	44.10	6.742	0	6.742	2.00	3.62	208.11
Heavy gas	65.49	8.198	0	8.198	2.53	3.74	228.51
Saturates	167.68	0	31.743	31.743	5.15	3.90	249.69
Aromatics + Resins (γ = 0.0)	253.79	0	9.907	9.907	6.41	3.99	285.00
Asphaltene	1700	0	0.133	0.133	33.00	4.20	353.50

Table 8
SARA analysis as reported by TLC-FID and HPLC for the crude oil B.

	TLC-FID	HPLC (IP 143)	HPLC/TLC-FID (P)
Saturates	49.5	73.0	1.47
Aromatics	40.2	19.1	0.48
Resins	7.2	7.6	1.06
Asphaltene	3.1	0.2	0.06

Table 9
SARA analysis corrected for crude oil C.

	TLC-FID	Corrected (=TLC-FID*P)	HPLC (IP 143)
Saturates	44.9	69.39	67.09
Aromatics	46.3	23.05	25.84
Resins	6.7	7.41	6.92
Asphaltene	2.1	0.14	0.15

by multiplying and renormalizing the crude oil C data with the corresponding ratio of HPLC/TLC-FID obtained from crude oil B. From Table 9, the corrected SARA is very close to the actual SARA measured by HPLC for crude oil C. Thus, under data constraints, such SARA estimations can be used for crude oils of similar nature and origin. Alternatively, the lost fraction during TLC-FID can be assumed to be composed of mostly the saturates (because of the higher volatility of saturates compared to aromatics and other components); and the actual SARA can be estimated by adding this lost fraction to the saturates reported in SARA and renormalizing.

6. Results and discussion

6.1. Pressure

The effect of pressure on asphaltene phase behavior can be explained by analyzing the depressurization of a model oil, where the toluene solution before combining with methane contains 1.0 g of asphaltene/100 ml toluene at 20 °C. During pressure depletion at constant temperature, asphaltene precipitate formation is observed within a range above and below the bubble point. In Fig. 5, as pressure drops during production from the reservoir pressure, the oil expands, reducing the oil solubility parameter, and becomes a poor solvent for asphaltene. At low enough pressure, the asphaltene precipitation onset is reached and asphaltene begins to precipitate. Upon further depressurization, the system arrives at its bubble point, where the light components, which are asphaltene precipitants, escape from the liquid phase. As this happens, the solubility parameter of the oil increases until the oil becomes a better asphaltene solvent.

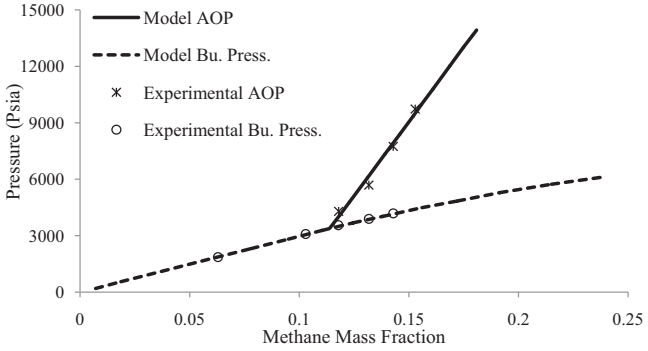

Fig. 5. PC-SAFT generated asphaltene phase diagram for a model oil composed of methane, toluene and asphaltene at 20 °C. Data from Ting et al. [48].

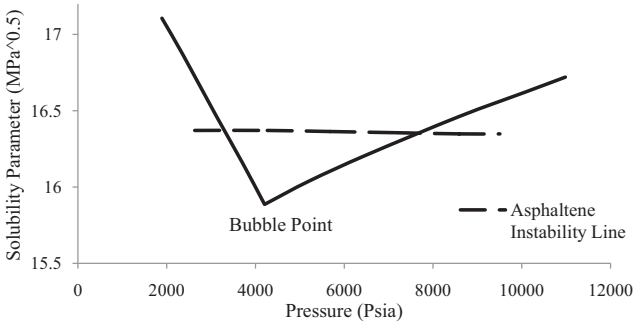

Fig. 6. PC-SAFT generated solubility parameter during pressure depletion for the model oil (methane, toluene and asphaltene) at 20 °C with 0.143 mass fraction methane above the bubble pressure.

The depressurization for the same system can be followed on a plot of solubility parameter as shown in Fig. 6 where asphaltene are unstable below the asphaltene instability line. In Fig. 6, the solubility parameter of oil decreases as the pressure is decreased to the bubble point. Upon further depressurization, the solubility parameter of oil increases. Thus, the maximum driving force for asphaltene precipitation is at the bubble point.

Please cite this article in press as: S.R. Panuganti, et al., SAFT model for upstream asphaltene applications, Fluid Phase Equilib. (2013), http://dx.doi.org/10.1016/j.fluid.2013.05.010

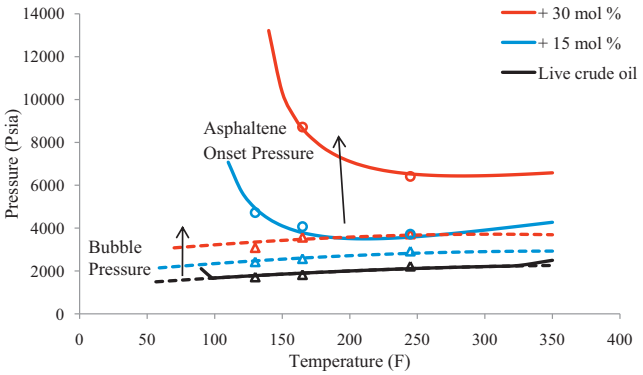

Fig. 7. Asphaltene phase behavior in crude oil B after the addition of natural gas. Injected gas composition (mol%): N_2-0.5%, CO_2-4.5%, C_1-87.4%, C_2-7.2% and C_3-0.4%.

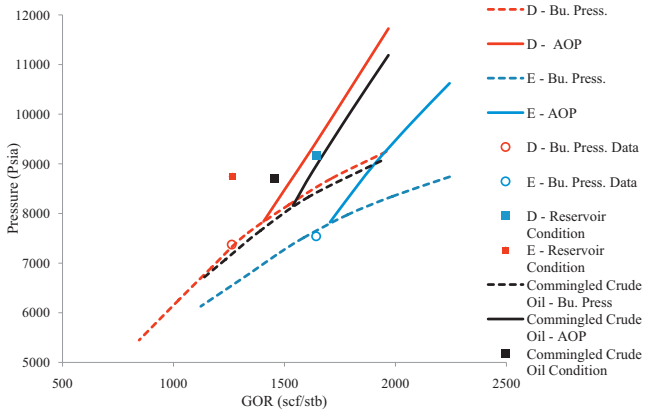

Fig. 8. PC-SAFT predicted asphaltene stability of commingled crude oils D and E in the volume ratio 50:50 at 150 F.

6.2. Temperature

The effect of temperature on asphaltene phase behavior can be explained by analyzing the phase diagram of crude oil A presented in Fig. 4. The nearly vertical phase boundary at about 130 F is an upper critical solution temperature phase boundary to the left of which asphaltene precipitate out of the crude oil. As the temperature rises above this boundary, the entropy gained from mixing just overcomes the enthalpically favored phase splitting and the system moves from a region of two liquid phases to a single liquid phase stable with asphaltene.

There is another phase boundary observed from Fig. 4 as the temperature is increased at constant pressure (e.g. at $P = 2500$ Psia and $T = 350$ F in Fig. 4). This is the phase boundary corresponding to lower critical solution temperature. As the temperature is increased at constant pressure, the crude oil expands lowering the solubility parameter of solvent and becomes a poor solvent for asphaltene. Prediction of this type of phase boundary requires an equation of state because it is the compressibility of the system that causes the phase splitting. The lower critical solution temperature phase boundary is more pronounced as the critical temperature of the crude oil is approached, because the system is most compressible in the critical region.

6.3. Gas injection

Changes in crude oil composition occur during gas injection processes employed in enhanced oil recovery, reservoir pressure maintenance and gas lift. The gas injection effect on asphaltene stability is studied by the addition of increasing amounts of natural gas at different temperature for crude oil B as shown in Fig. 7. The PC-SAFT predictions match the experimental observations of both the asphaltene onset and bubble pressures for varying amount of the natural gas injected into the live oil. The dissolved gas decreases asphaltene solubility and the asphaltene become more unstable. Thus along with an increasing trend of bubble pressure (due to more volatiles) asphaltene onset pressure also increases. Specific effects on asphaltene precipitation onset due to CO_2, N_2 and methane injection also show an increasing asphaltene instability with increasing injection of the gases amount [68].

6.4. Comingling of crude oils

Changes in composition also arise from the relative proportions of mixing fluids. Reducing the number of flow lines by commingling streams from several wells or manifolds is a common subsea design consideration. This decision can reduce capital and operational costs, but might cause problems if the fluids in the streams are not compatible with respect to asphaltene. A mixture of different oil streams can generate asphaltene precipitation. This problem might occur when fluids of very different API gravities are mixed. For example, when condensate is mixed with black oil. The density of the entire liquid phase decreases, reducing the crude oil solubility parameter and the asphaltene precipitate.

The effect of mixing crude oils on asphaltene phase behavior can be analyzed by considering comingling of two crudes oils D and E as shown in Fig. 8. None of these fluids show asphaltene instability at their corresponding reservoir condition. During pressure depletion, asphaltene precipitation is not expected to occur for any of the fluids at their respective reservoir temperature and gas-to-oil ratio. Asphaltene would precipitate only above their reservoir gas-to-oil ratio. However, crude oil E is unstable in asphaltene with respect to the reservoir conditions of crude oil D and the resultant commingled oil is a good case to study the effect of crude oils commingling on asphaltene instability. The crude oils when combined in equal volume, Fig. 8 show the PC-SAFT predicted asphaltene phase behavior of the commingled system. The asphaltene precipitation is not expected to occur at the mixture gas-to-oil ratio of 1453 scf/stb which is consistent with the field observations.

6.5. Oil based mud

Oil based mud (OBM) which is used to increase borehole stability during drilling can contaminate the near wellbore reservoir fluids. Significant overbalance pressure during the drilling process can result in mud invasion into the formation and mix with the reservoir fluid. An oil based mud can significantly modify oil composition and predicted phase behavior of asphaltene in the formation fluid leading to wrong interpretation of the data.

Oil based mud being a precipitating agent for asphaltene is expected to increase the pressure at which asphaltene start precipitating. Simulations using the PC-SAFT equation of state performed for a clean and OBM contaminated oil show that this is not necessarily the case. According to the results presented in Fig. 9, for a crude oil F, both the asphaltene precipitation onset and bubble pressure decrease when successive amount of oil based mud are added [62]. The asphaltene onset pressure and the bubble point curves estimated by PC-SAFT closely follow the experimental findings. A decrease in the gas-to-oil ratio due to oil based mud addition is also noted. Although the oil based mud is a precipitant for asphaltene, the OBM contamination dilutes the gaseous components of the oil that are stronger asphaltene precipitants. As the gas-to-oil ratio decreases, the asphaltene precipitation onset pressure and bubble point pressure decrease. The correction for oil based mud contamination can be significant in the temperature range of the production as observed from Fig. 10 for the same crude oil F [62].

Please cite this article in press as: S.R. Panuganti, et al., SAFT model for upstream asphaltene applications, Fluid Phase Equilib. (2013), http://dx.doi.org/10.1016/j.fluid.2013.05.010

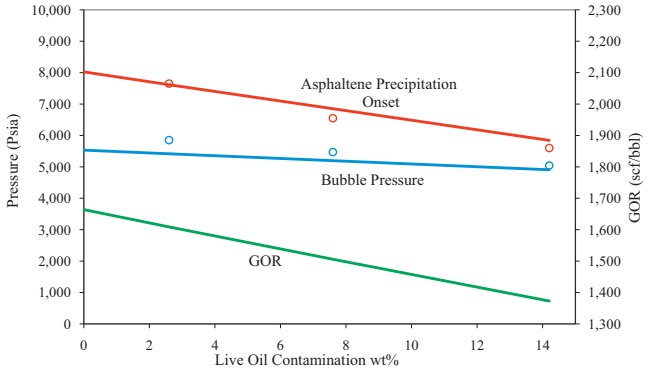

Fig. 9. PC-SAFT simulation of oil based mud contamination effect on the asphaltene phase behavior of crude oil F at 178 F.

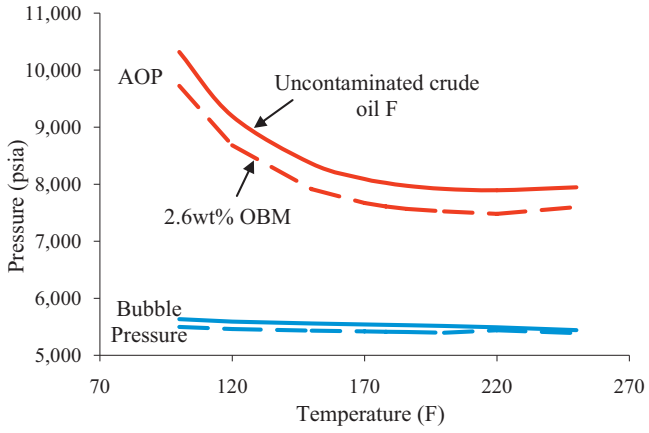

Fig. 10. Asphaltene phase behavior of crude oil F calculated with the PC-SAFT.

6.6. Asphaltene polydispersity

The effect of asphaltene's polydispersity on its phase behavior can be analyzed by modeling the polydisperse asphaltene using PC-SAFT. The experimental data for polydispersity modeling is obtained from the titration results of crude oil G presented by Hirschberg et al. [42]. For modeling these stock tank oil dilution experiments with n-alkanes, asphaltene fraction in the characterization process is divided into three sub-fractions: n-C_{5-7}, n-C_{7-10} and n-C_{10+} asphaltene, based on the experimental amount of n-C_5, n-C_7 and n-C_{10} asphaltene obtained upon addition of n-pentane, n-heptane and n-decane, respectively. The molecular weight of each of the asphaltene sub-fractions is different, and is discussed in the supplementary section on how the polydisperse asphaltene parameters are estimated.

A comparison of the PC-SAFT equation of state generated and the experimental data for onset and amount of asphaltene precipitation are shown in Figs. 11 and 12, respectively. Titration experiments presented by Hirschberg et al. contains onset of precipitation for four different n-alkanes as well as precipitation amount for three different titration agents. PC-SAFT mass distribution plots of the asphaltene sub-fractions as a function of dilution ratio are shown in Fig. 13 when n-pentane, n-heptane and n-decane are used as the precipitating agents, respectively. As seen in Fig. 13, near the initial asphaltene instability onset, the precipitated phase is composed mostly of the heaviest asphaltene fractions (n-C_{10+} sub-fraction). As the amount of precipitant is increased further, lower molecular weight asphaltene will precipitate.

From Fig. 13, a decreasing amount of asphaltene precipitate is observed with high dilution ratios, a phenomenon verified by Wang

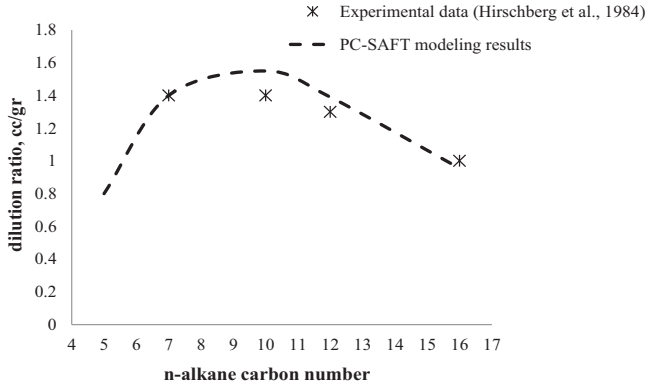

Fig. 11. Comparison of the PC-SAFT and the asphaltene instability onset experimental data for crude oil G.

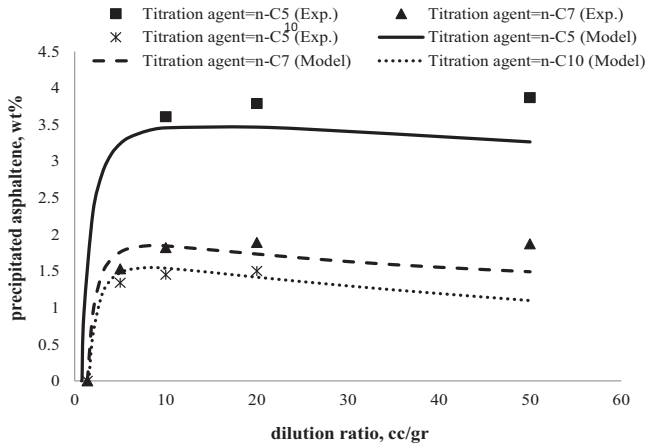

Fig. 12. Comparison of the PC-SAFT and the experimental amount of precipitated asphaltene for crude oil G.

and Buckley [69]. This is happening because; any precipitate can redissolve thermodynamically at very high dilution in a precipitant. The amount of dilution that is "high enough" for asphaltene depends upon the highest molecular-weight components of the asphaltene fraction. From Fig. 13, one can observe that rate of redissolution is most for C_{5-7} asphaltene sub-fraction, because it is the lightest asphaltene sub-fraction and has the lowest molecular weight value.

6.7. Asphaltene phase behavior modeling by cubic and PC-SAFT EoS

Despite their poor prediction of liquid properties, cubic equations of state are widely used in the petroleum industry due to the simplicity of the models. In the thermodynamic modeling of asphaltene, it is seen that the parameters fit using a cubic equation of state for a particular data set fails to predict another situation for the same well [70]. This is demonstrated in Fig. 14 where the parameters for both SRK-P and PC-SAFT are estimated to the saturation pressures and asphaltene onset pressures for various temperature of crude oil H with 5 mol% gas injection. The same parameters are then used to predict the saturation pressure and temperature dependence of the asphaltene onset pressure for different amounts of gas injected. The predictions made by the PC-SAFT and cubic equation of state are compared in Fig. 14A, C and D. It is observed that only PC-SAFT does a good job in predicting the phase behavior of asphaltene even with compositional changes.

The major limitation of any cubic equation of state is that they cannot describe adequately the phase behavior of mixtures of

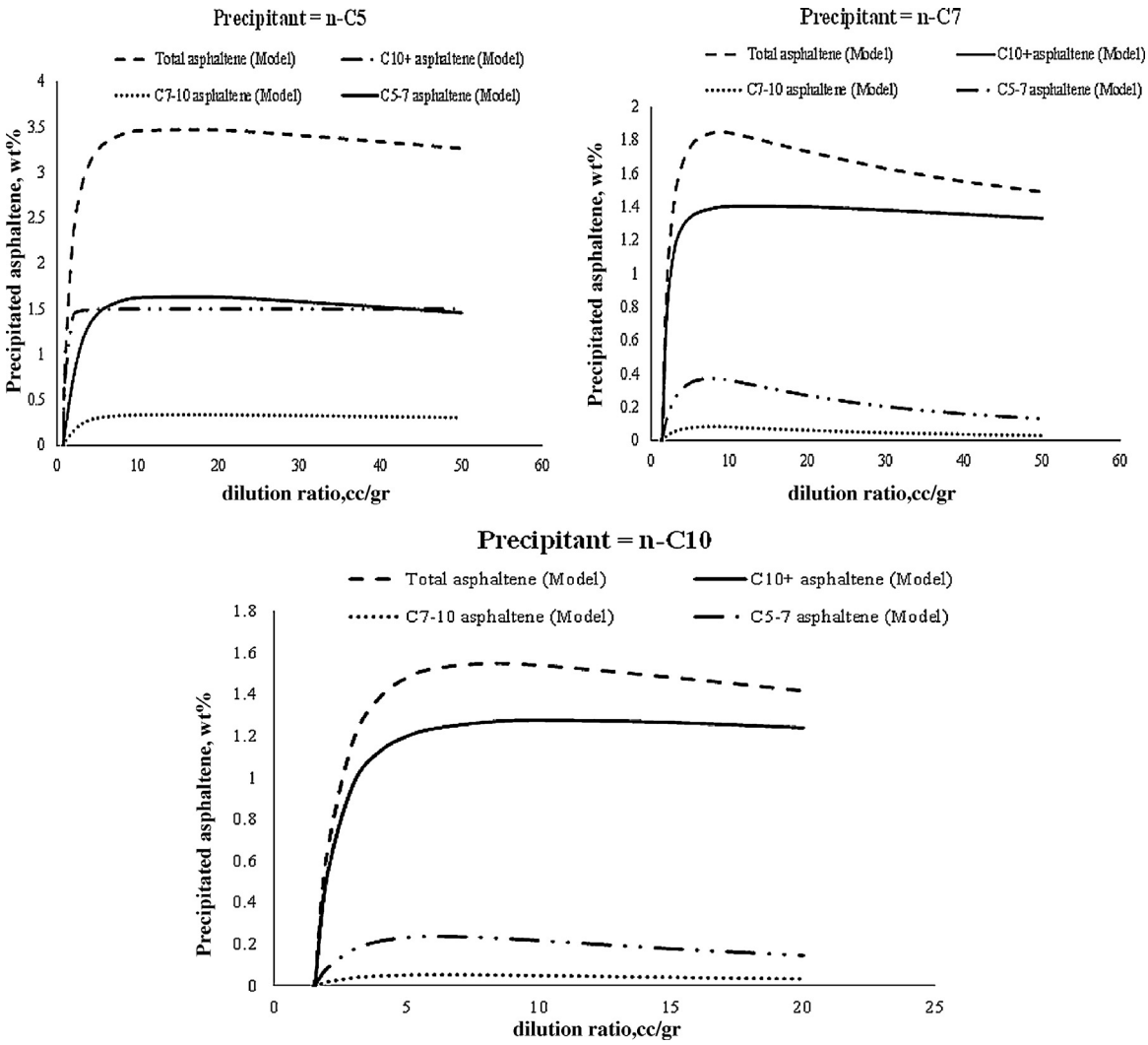

Fig. 13. Distribution of the asphaltene sub-fractions in the precipitated phase as a function of n-pentane, n-heptane and n-decane dilution ratio in crude oil G.

molecules with large size differences and they are unable to accurately calculate liquid densities of the precipitated phase. Accurate modeling of liquid density is essential for an equation of state to predict liquid–liquid equilibrium and their corresponding parameters, such as the solubility parameter, over a range of conditions.

The association term from SAFT can be added to a cubic equation of state to produce a non-cubic model called as the cubic plus association equation of state [71]. This cubic plus association equation of state has been applied for asphaltene phase behavior with some success. However, this model requires a lot more parameters than SAFT, and for a nonassociating system reduces to the simple cubic equation of state with the same drawbacks.

6.8. Asphaltene composition gradients

Fluid properties vary along the depth of a continuous reservoir due to the gravitational field, an effect called compositional grading. A considerable elevation difference produces the thermodynamic drive creating the composition gradient [72]. A resultant of the compositional grading is greater gas-to-oil ratio from the upper parts of a formation. With the fluid being well characterized at a particular depth, the Whitson's compositional grading algorithm is used to analyze the compositional grading related to asphaltene using PC-SAFT equation of state [73].

The use of PC-SAFT for asphaltene compositional grading can be understood by considering the case of Tahiti reservoir. For the Tahiti field in the Gulf of Mexico, Fig. 15 shows the changes in asphaltene amount (measured in terms of optical density) with depth which could result from the attainment of thermodynamic equilibrium in a uniform gravitational field as predicted by PC-SAFT and compared with field data. The field data is obtained from down-hole fluid analysis by measuring the optical density using infrared light. A close match is observed between the predicted asphaltene concentration gradient and the field data procured by down-hole fluid analysis. This asphaltene compositional gradient can be further used to evaluate the connectivity of wells and reservoir compartmentalization by following the analysis of Mullins [74].

6.9. Tar-Mat

Asphaltene compositional gradient can lead to significant variations in crude oil viscosity and extreme cases of asphaltene compositional grading can lead to tar-mat formation [75]. Tar-mat represents a reservoir zone of highly viscous extra heavy oil enriched with asphaltene relative to oil column [76]. A tar-mat is differentiated from heavy oil in that the tar-mat is characterized by high oil saturation associated with high residual oil saturation during logging [77].

Please cite this article in press as: S.R. Panuganti, et al., SAFT model for upstream asphaltene applications, Fluid Phase Equilib. (2013), http://dx.doi.org/10.1016/j.fluid.2013.05.010

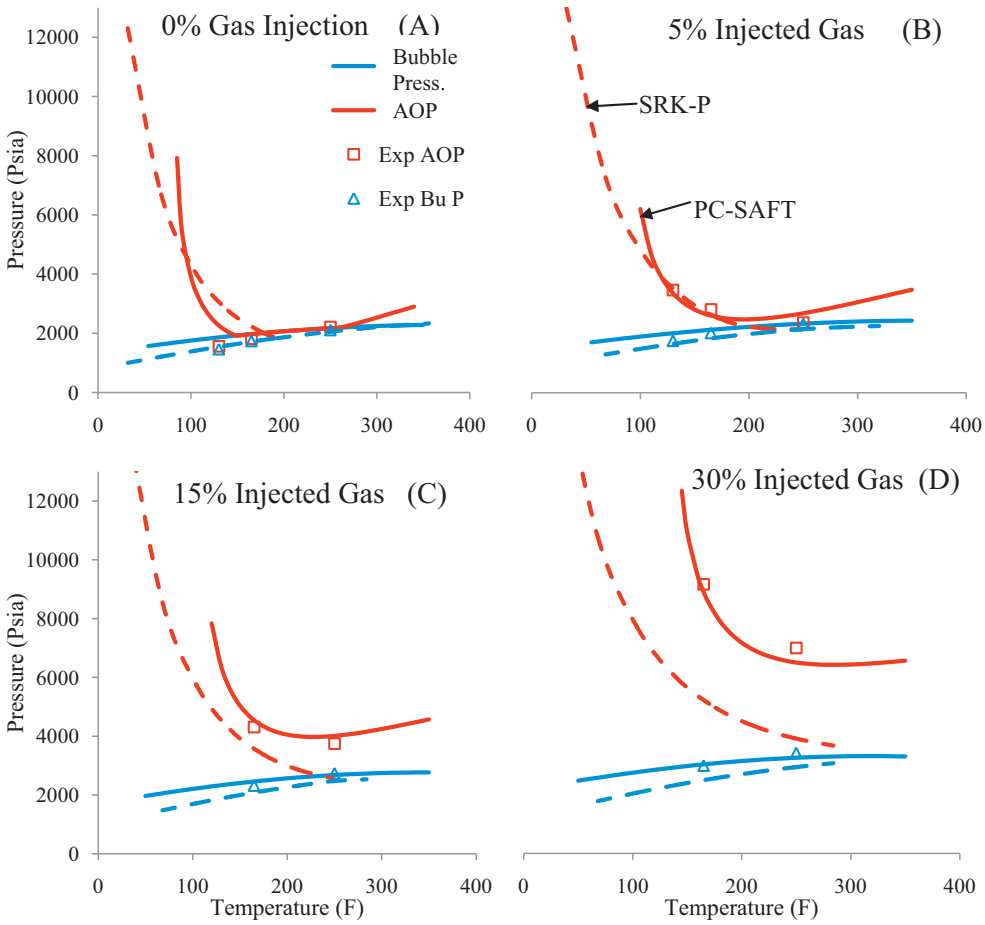

Fig. 14. PC-SAFT and SRK-P phase behavior predictions for crude oil H after estimating the parameters for 5 mol% of gas injection data. Injected gas composition (mole %): N_2-0.4%, CO_2-3.9%, C_1-71.4%, C_2-12%, C_3-7.2%, heavy gas-5.1%.

The reservoir considered for tar-mat study is the field A consisting of crude oil A. The tar-mat can be formed by any of the mechanisms such as, biodegradation at oil–water contact, gas diffusion, oil cracking or flocculation of precipitated asphaltene. But as long as the tar-mat is in thermodynamic equilibrium with the rest of the reservoir fluid, the plot of asphaltene content with depth should be able to detect the tar-mat formation depth as a sharp transition in the asphaltene amount. The PC-SAFT asphaltene compositional grading when extended to further depths to model the possibility of this tar-mat formation resulted in Fig. 16 for field A. After a depth of ~9050 ft in the model, the asphaltene content suddenly increased from 15 wt% to 48 wt%. Asphaltene measurements of the tar-mat samples report between 26 and 80 weight percent [78]. Above 9000 ft asphaltene is stable in the oil even with increasing asphaltene content with depth. But by 9050 ft, asphaltene concentration increased to an extent of phase separation. Thus, the tar-mat formed can be explained in terms of the transport of asphaltene in oil along chemical and gravitational potential gradients in the reservoir to the zone of asphaltene enrichment at the site of tar-mat.

The PC-SAFT observed tar-mat formation is in accordance with the field observation of tar-mat depth (Fig. 17) and the asphaltene content of the tar-mat. Hence, the PC-SAFT model successfully predicted the tar-mat occurrence depth from just knowing the pressure, temperature and reservoir oil composition at a reference depth in the upper parts of the formation. Such a prediction

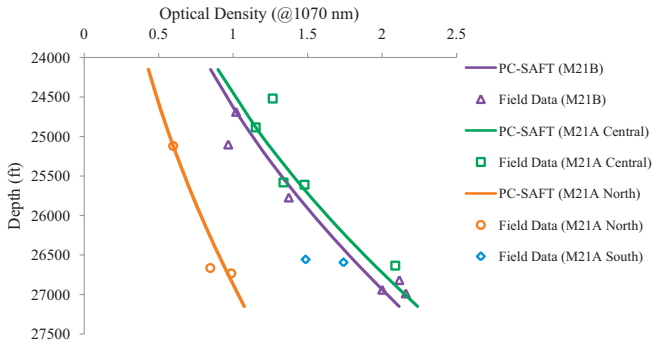

Fig. 15. PC-SAFT generated optical density profile of Tahiti crude oil with depth in the Tahiti field at the reservoir temperature of 200 F.

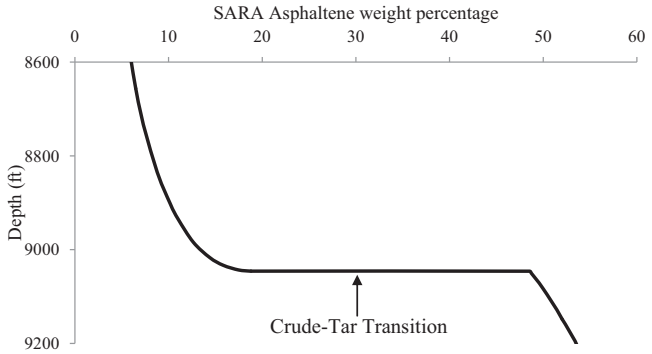

Fig. 16. PC-SAFT prediction of tar-mat in the field A consisting of crude oil A.

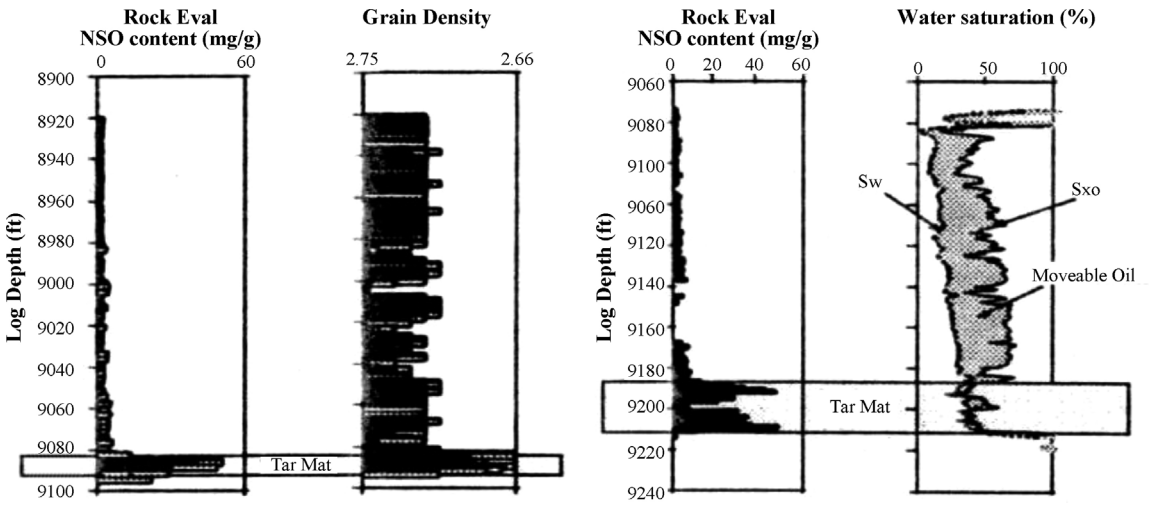

Fig. 17. The figures are well logs from two different wells identifying the tar-mat in field A.

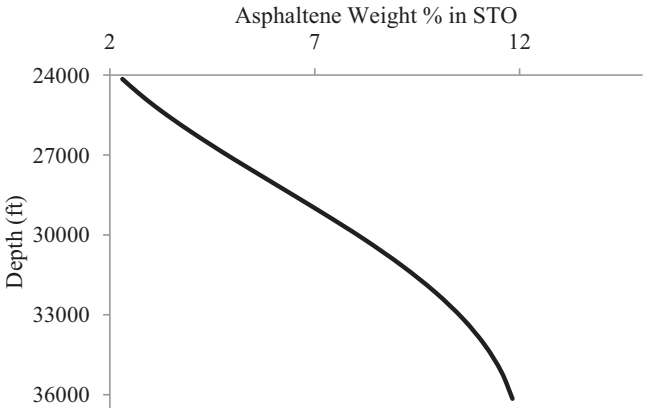

Fig. 18. Asphaltene compositional variation with depth in the Tahiti field generated by PC-SAFT indicates no tar-mat.

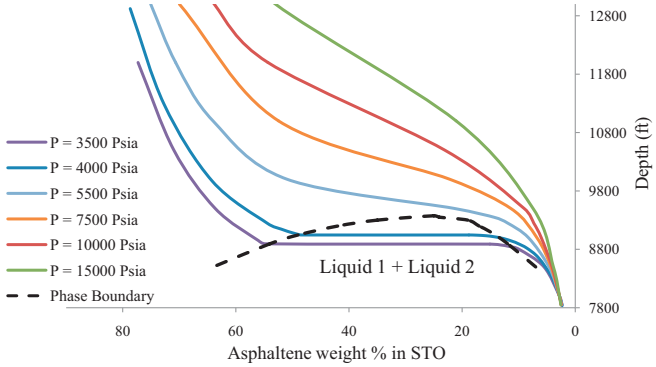

Fig. 19. Asphaltene compositional grading isotherms with different starting pressures at the reference depth of 8000 ft (Liquid 1: ashaltene lean phase, Liquid 2: asphaltene rich phase).

is possible only with an equation of state, because along with asphaltene phase splitting the compressibility of oil needs to be taken into consideration.

6.9.1. Tar-mat analysis

The Tahiti field asphaltene compositional grading curve, when extended to deeper depths using PC-SAFT, does not show any kink in the curve; indicating no presence of a tar-mat (Fig. 18) corroborated by the field operations. But the field A showed a sharp asphaltene compositional variation correlating to a tar-mat. Recently Zuo et al. have reported observing large asphaltene gradients even without asphaltene instabilities for a field in Middle East [79]. Thus a general analysis on when asphaltene show large compositional contrasts is needed.

In the field A, PC-SAFT asphaltene compositional grading plots generated with different starting pressures at the reference depth, 8000 ft are plotted together in Fig. 19. The sharp compositional contract represents tar-mat formation depth where the crude oil is phase splitting into two liquid phases (asphaltene lean and rich phases) existing at equilibrium. The boundaries of these liquid–liquid phase separations when joined using the discontinuous black line represents the phase boundary and is analogues to PV isotherms. Observed from Fig. 18, as one approaches the critical point region on this composition-depth phase diagram, there exists sharp asphaltene compositional gradients even without phase transitions. Thus it is can be concluded that, there need not be phase separation to have large compositional gradients and, based on the system's instability to asphaltene the tar-mat formation depth and the asphaltene content in tar-mat vary.

7. Conclusions

Asphaltene constitute a potential problem in oil production because of the tendency of this petroleum fraction to precipitate and deposit. Predicting asphaltene flow assurance issues requires the ability to model phase behavior of asphaltene as a function of the operating conditions. In this work a modeling method based on the PC-SAFT equation of state is presented, in which for a given crude oil, a single set of simulation parameters is sufficient to predict the phase behavior with various compositional changes. Among the experimental information necessary to fit the simulation parameters, SARA requires special attention because, measurements performed using different techniques can lead to results that are significantly different. A methodology to correct the SARA values is presented, which seems to provide satisfactory results for the case of light crude oils of similar nature.

The PC-SAFT equation of state is successful in modeling the phase stability of asphaltene in crude oil over a wide range of conditions and for a variety of cases, including:

- Effect of pressure: In reservoir depressurization, there is a pressure range where asphaltene become unstable. As the pressure decreases along the wellbore, oil expands making it a poor solvent

Please cite this article in press as: S.R. Panuganti, et al., SAFT model for upstream asphaltene applications, Fluid Phase Equilib. (2013), http://dx.doi.org/10.1016/j.fluid.2013.05.010

for asphaltene. Eventually, asphaltene undergo a phase separation, at a pressure that is known as the asphaltene onset pressure. As the pressure keeps decreasing the bubble point is reached, and the light fraction of hydrocarbons, which are strong asphaltene precipitants, escape from the liquid phase. As this happen, asphaltene become stable again.

- Effect of temperature: At a given pressure, asphaltene can become stable or unstable by increasing the temperature depending on the location of the system on the phase diagram. At low temperature, asphaltene can get re-dissolved by increasing the temperature because the entropy gain overcomes the enthalpically favored phase splitting. However, at much higher temperature, the volume of the oil increases making it a poor solvent for asphaltene and causing their phase separation. The latter case might explain the fouling of heat exchangers produced during the refining process.
- Gas addition: An increase of asphaltene onset pressure and bubble point is observed upon the addition of miscible gas, which decreases the solubility of asphaltene. The prediction of asphaltene precipitation onset and bubble pressure is satisfactory for all the gas percentages tested.
- Commingling of crude oils: A mixture of incompatible oils might induce the precipitation of asphaltene. For the case of crude oils D and E, the asphaltene phase behavior of the commingled system did not show instability towards asphaltene. An extreme mixing condition for asphaltene instability might be when a gas condensate is mixed with black oil.
- Oil based mud contamination: Although at first it is expected that the contamination with oil based mud will increase the instability of asphaltene, it is confirmed that this is not the case. The addition of oil based mud dilutes the light fractions present in the live oil, making the asphaltene stabilized. The PC-SAFT equation of state correctly predicts this phenomenon, and the simulation results obtained match well with the available data.

Furthermore, results on the effect of asphaltene polydispersity are presented, and is observed that higher molecular weight asphaltene precipitate first followed by lighter asphaltene subfractions upon further precipitation. Finally, isothermal asphaltene compositional grading is analyzed from knowing just pressure, temperature and composition in the upper farts of a formation. The PC-SAFT generated asphaltene compositional grading showed a close agreement with the field data. Compositional grading can lead to significant variations in crude oil properties and in some cases to the formation of a tar-mat. A novel representation of the tar-mat formation produced by asphaltene compositional grading is presented in the form of a composition–depth phase diagram. The sharp compositional contract represents tar-mat formation depth, where the crude oil is phase splitting into two liquid phases (asphaltene lean and rich phases), which co-exist at equilibrium. The tar-mat formation depth and the asphaltene content in a tar-mat vary based on the extent of asphaltene's instability in a crude oil.

In overall, the modeling method for asphaltene phase behavior presented in this article is clearly very versatile and offers great potential for the design of improved experimental procedures and for a better understanding of the asphaltene behavior observed in the daily operations of oil fields across the world.

Acknowledgments

This work is undertaken with the funding from the R&D Oil Subcommittee of the Abu Dhabi National Oil Company. The authors are thankful to Shahin Negahban, Dalia Abdullah, Sanjay Misra and the Enhanced Oil Recovery Technical Committee for valuable data and support. The authors also thank Oliver Mullins, Jefferson Creek and George Hirasaki for helpful discussions. The authors thank the technical committee of "The 1st International Conference on Upstream Engineering and Flow Assurance" and UE & FA Forum for inviting the presentation of this work.

Appendix A.

Details of crude oils used in the current study are listed below. Crude oil C is not used for asphaltene modeling work, and hence its properties are not reported. Properties of the crude oils D and E cannot be reported due to proprietary data. Titration experiments to understand the asphaltene polydispersity were carried out on dead oil by Hirschberg et al. All the other oils used in this study are live oils.

	Crude oil A	Crude oil B	Crude oil F	Crude oil G	Crude oil H	Tahiti crude oil
GOR (scf/stb)	787	852	1664	–	798	510
MW of reservoir fluid (g/mol)	97.75	92.78	70.27	–	96.15	131.5
MW of flashed gas (g/mol)	29.06	30.24	22.59	–	28.54	25.83
MW of STO (g/mol)	192.99	182.02	227.58	221.50	191.02	243.26
STO Density (g/cm^3)	0.820	0.817	0.862	0.873	0.823	0.880
Saturates (wt%)	66.26	73.42	52.30	n-C_5 asphaltene, wt% = 3.90	75.56	52.90
Aromatics (wt%)	25.59	19.32	28.00	n-C_7 asphaltene, wt% = 1.90	20.08	29.70
Resins (wt%)	5.35	7.05	11.30	n-C_{10} asphaltene, wt% = 1.40	4.14	13.20
Asphaltene (wt%)	2.80	0.17	8.40	Asphaltene + Resin, wt% = 18.00	0.22	4.00

Please cite this article in press as: S.R. Panuganti, et al., SAFT model for upstream asphaltene applications, Fluid Phase Equilib. (2013), http://dx.doi.org/10.1016/j.fluid.2013.05.010

Appendix B. Supplementary data

Supplementary data associated with this article can be found, in the online version, at http://dx.doi.org/10.1016/j.fluid.2013.05.010.

References

[1] M. Boussignault, Ann. Chim. Phys. 2 (1837) 64–141.
[2] T.F. Yen, in: O.C. Mullins, E.Y. Sheu (Eds.), Structures and Dynamics of Asphaltenes, Plenum Press, New York, 1998, pp. 1–20.
[3] T.F. Yen, Prepr. Am. Chem. Soc. Div. Pet. Chem. 17 (1972) F102.
[4] J. Murgich, J.A. Abaner, Energy Fuels 13 (1999) 278–288.
[5] O.C. Mullins, Energy Fuels 24 (2010) 2179–2207.
[6] D. Espinat, E. Rosenberg, M. Scarsella, L. Barre, D. Fenistein, D. Broseta, in: O.C. Mullins, E.Y. Sheu (Eds.), Structures and Dynamics of Asphaltenes, Plenum Press, New York, 1998, pp. 145–202.
[7] F.M. Vargas, Department of Chemical and Biomolecular Engineering Seminar Series, April 2, Houston, USA, 2013.
[8] J.P. Dickie, T.F. Yen, Anal. Chem. 39 (1967) 1847–1852.
[9] P.M. Spiecker, K.L. Gawrys, P.K. Kilpatrick, J. Colloid Interface Sci. 267 (2003) 178–193.
[10] H. Alboudwarej, K. Akbarzedeh, J. Beck, W.Y. Svrcek, H.W. Yarranton, AICHE J. 49 (2003) 2948–2956.
[11] J.Y. Zuo, O.C. Mullins, D. Chengli, D. Zhang, Nat. Resour. 1 (2010) 19–27.
[12] A. Hirschberg, L.J.P.C.M. Hermans, International Symposium on Characterization of Heavy Crude Oils and Petroleum Residues, June 25–27, Lyon, France, 1984.
[13] H.W. Yarranton, J.H. Masliyah, AICHE J. 42 (1996) 3533–3543.
[14] M. Nomura, S. Murata, K. Kidena, T. Ookawa, H. Komoda, Fuel Chem. Divis. Prepr. 48 (2003) 46–47.
[15] E. Rogel, L. Carbognani, Energy Fuels 17 (2003) 378–386.
[16] M.S. Diallo, T. Cagin, J.L. Faulon, W.A.W.A. Goddard, in: G.V. Chilingar, T.F. Yen (Eds.), Asphaltenes and Asphalts, vol. 2, Elsevier, 2000, pp. 103–128.
[17] T.F. Yen, J.G. Erdman, W.E. Hanson, J. Chem. Eng. Data 6 (1961) 443–448.
[18] J.A. Ostlund, J.E. Lofroth, K. Holmberg, M. Nyden, J. Colloid Interface Sci. 253 (2002) 150–158.
[19] J.A. Ostlund, S.I. Andersson, M. Nydén, Fuel 80 (2001) 1529–1533.
[20] M. Jeribi, A.B. Almir, D. Langevin, I. Henaut, J.F. Argillier, J. Colloid Interface Sci. 256 (2002) 268–272.
[21] F. Bauget, D. Langevin, R. Lenormand, J. Colloid Interface Sci. 239 (2001) 501–508.
[22] B.B. Maini, H.K. Sarma, A.E. George, J. Can. Petrol. Technol. 32 (1993) 50–54.
[23] L. Liggieria, F. Raverab, M. Ferraria, A. Passeronea, R. Miller, J. Colloid Interface Sci. 186 (1997) 46–52.
[24] E.B. Sirota, M.Y. Lin, Energy Fuels 25 (2007) 2809–2815.
[25] J. Escobedo, G.A. Manaoori, SPE J. (1996) SPE28729.
[26] A. Hirschberg, J. Petrol. Technol. 40 (1998) 89–94.
[27] J.X. Wang, J.S. Buckley, Energy Fuels 15 (2001) 1004–1012.
[28] J.S. Buckley, Energy Fuels 13 (1999) 328–332.
[29] A. Khoshandam, A. Alamdari, Energy Fuels 24 (2010) 1917–1924.
[30] I.K. Yudin, G.L. Nikolaenko, E.E. Gorodetskii, E.L. Markhashov, V.A. Agayan, M.A. Anisimov, J.V. Sengers, Physica A 251 (1998) 235–244.
[31] M.A. Anisimov, I.K. Yudin, V. Nikitin, G. Nikolaenko, A. Chernoutsan, H. Toulhoat, D. Frot, Y. Briolant, J. Phys. Chem. 99 (1995) 9576–9580.
[32] S. Acevedo, J. Castillo, A. Fernández, S. Goncalves, M.A. Ranaudo, Energy Fuels 12 (1998) 386–390.
[33] A. Rudrake, K. Karan, J.H. Horton, J. Colloid Interface Sci. 332 (2009) 22–31.
[34] S. Acevedo, M.A. Ranaudo, C. García, J. Castillo, A. Fernández, M. Caetano, S. Goncalves, Colloids Surf. A: Physicochem. Eng. Aspects 166 (2000) 145–152.
[35] L. Nabzar, M.E. Aguiléra, Oil Gas Sci. Technol. 63 (2008) 21–35.
[36] F.M. Vargas, S.R. Panuganti, F. Yap, J. Chai, W.G. Chapman, SPE ATW Flow Assurance and Production Chemistry—Integration of Disciplines to Address the Challenges of Tomorrow, May 30–June 1, Dubai, UAE, 2011.
[37] L. Goual, 10th International Conference on Petroleum Phase Behavior and Fouling, June 14–18, Rio de Janeiro, Brazil, 2009.
[38] J. Czarnecki, 10th International Conference on Petroleum Phase Behavior and Fouling, June 14–18, Rio de Janeiro, Brazil, 2009.
[39] S. Priyanto, A.G. Mansoori, A. Suwono, Chem. Eng. Sci. 56 (2001) 6933–6939.
[40] L.X. Nghiem, D.A. Coombe, Soc. Pet. Eng. J. 2 (1997) 170–176, SPE 36106.
[41] J. Wu, J.M. Prausnitz, A. Firoozabadi, AICHE J. 46 (2000) 197–209.
[42] A. Hirschberg, L.N.J. Dejong, B.A. Schipper, J.G. Meijer, SPE J. 24 (1984) 283–293.
[43] W.G. Chapman, S.G. Sauer, D. Ting, A. Ghosh, Fluid Phase Equilibr. 217 (2004) 137–143.
[44] W.G. Chapman, K.E. Gubbins, G. Jackson, M. Radosz, Fluid Phase Equilibr. 52 (1989) 31–38.
[45] W.G. Chapman, K.E. Gubbins, G. Jackson, M. Radosz, Ind. Eng. Chem. Res. 29 (1990) 1709–1721.
[46] W.G. Chapman, G. Jackson, K.E. Gubbins, Mol. Phys. 65 (1998) 1057–1079.
[47] I.G. Economou, Ind. Eng. Chem. Res. 41 (2002) 953–962.
[48] D. Ting, G.J. Hirasaki, W.G. Chapman, Petrol. Sci. Technol. 21 (2003) 647–661.
[49] J. Gross, G. Sadowski, Ind. Eng. Chem. Res. 40 (2001) 1244–1260.
[50] G.A. Mansoori, N.F. Carnahan, K.E. Starling, T.W. Leland, J. Chem. Phys. 54 (1971) 1523–1525.
[51] S.S. Chen, A. Kreglewski, Ber. Bunsenges. Phys. Chem. 81 (1977) 1048–1052.
[52] J.A. Barker, D. Henderson, J. Chem. Phys. 47 (1967) 4714–4721.
[53] J.S. Buckley, G.J. Hirasaki, Y. Liu, S. Von Drasek, J.X. Wang, B.S. Gill, Petrol. Sci. Technol. 16 (1998) 251–285.
[54] D.L. Katz, A. Firoozabadi, J. Petrol. Technol. 30 (1978) 1649–1655.
[55] H.P. Roenningsen, I. Skjevrak, E. Osjord, Energy Fuels 3 (1989) 744–755.
[56] C.H. Whitson, SPE J. 23 (1983) 683–694.
[57] M.R. Riazi, T.E. Daubert, Hydrocarbon Process. 60 (1980) 115–116.
[58] M.R. Riazi, Characterization and Properties of Petroleum Fractions, ASTM, Philadelphia, 2005.
[59] M.R. Riazi, A. Taher, Fluid Phase Equilibr. 117 (1996) 217–224.
[60] P. Leelavanichkul, M.D. Deo, F.V. Hanson, Petrol. Sci. Technol. 22 (2004) 973–990.
[61] K.S. Pedersen, P.L. Christensen, Phase Behavior of Petroleum Reservoir Fluids, CRC Press, Boca Raton, 2007.
[62] D.L. Gonzalez, G.J. Hirasaki, W.G. Chapman, Energy Fuels 21 (2007) 1231–1242.
[63] D.L. Gonzalez, D. Ting, G.J. Hirasaki, W.G. Chapman, Energy Fuels 19 (2005) 1230–1234.
[64] S.R. Panuganti, F.M. Vargas, D.L. Gonzalez, A.S. Kurup, W.G. Chapman, Fuel 93 (2012) 658–669.
[65] S. Punnapala, F.M. Vargas, Fuel 108 (2013) 417–429.
[66] T. Fan, J.S. Buckley, Energy Fuels 16 (2002) 1571–1575.
[67] A.M. Kharrat, J. Zacharia, V.J. Cherian, A. Anyatonwu, Energy Fuels 21 (2007) 3618–3621.
[68] D.L. Gonzalez, F.M. Vargas, G.J. Hirasaki, W.G. Chapman, Energy Fuels 22 (2008) 757–762.
[69] J. Wang, J. Buckley, J. Dispers. Sci. Technol. 28 (2007) 425–430.
[70] W.G. Chapman, S.R. Panuganti, A.S. Kurup, AIChE/SPE Joint Workshop on Challenges in Flow Assurance, September 26–28, Houston, USA, 2011.
[71] G.M. Kontogeorgis, E.C. Voutsas, I.V. Yakoumis, D.P. Tassios, Ind. Eng. Chem. Res. 35 (1996) 4310–4318.
[72] S.R. Panuganti, F.M. Vargas, W.G. Chapman, Energy Fuels 26 (2012) 2548–2557.
[73] C.H. Whitson, U. Trondheim, P. Belery, Centennial Petroleum Symposium, Tulsa, USA, SPE 28000, 1994.
[74] O.C. Mullins, The Physics of Reservoir Fluids: Discovery through Downhole Fluid Analysis, 1st ed., Schlumberger, Houston, 2008.
[75] B. Carpentiera, H. Arab, E. Pluchery, J.M. Chautru, J. Petrol. Sci. Eng. 58 (2007) 472–490.
[76] A. Wilhelms, B. Carpentier, A.Y. Huc, J. Petrol. Sci. Eng. 12 (1994) 147–155.
[77] A. Wilhelms, S.R. Larter, Marine Petrol. Geol. 11 (1994) 418–441.
[78] M.N.D. Kaye, ADCO Proprietary Rep. (2006).
[79] J.Y. Zuo, O.C. Mullins, V.K. Mishra, G. Garcia, C. Dong, D. Zhang, Energy Fuels 26 (2012) 1670–1680.